

## RESEARCH ARTICLE

# Tamoxifen reduces silicone implant capsule formation in a mouse model

Kevin M. Blum<sup>1,2</sup>  | Gabriel J. M. Mirhaidari<sup>1,3</sup> | Jacob C. Zbinden<sup>1,2</sup> | Christopher K. Breuer<sup>1</sup> | Jenny C. Barker<sup>1,4</sup> 

<sup>1</sup>Center for Regenerative Medicine, The Abigail Wexner Research Institute, Nationwide Children's Hospital, Columbus, Ohio, USA

<sup>2</sup>Department of Biomedical Engineering, The Ohio State University, Columbus, Ohio, USA

<sup>3</sup>Biological Sciences Graduate Program, The Ohio State University, Columbus, Ohio, USA

<sup>4</sup>Department of Plastic and Reconstructive Surgery, Wexner Medical Center, The Ohio State University, Columbus, Ohio, USA

## Correspondence

Jenny C. Barker, Center for Regenerative Medicine, The Abigail Wexner Research Institute, Nationwide Children's Hospital, Columbus OH, USA.  
Email: [jenny.barker@osumc.edu](mailto:jenny.barker@osumc.edu)

## Abstract

Capsular contracture as a result of the foreign body response (FBR) is a common issue after implant-based breast reconstruction, affecting up to 20% of patients. New evidence suggests that tamoxifen may mitigate the FBR. C57BL/6 female mice were treated with daily tamoxifen or control injections and implanted with bilateral silicone implants in the submammary glandular plane. Implants were removed *en bloc* after 2 weeks and the implant capsules were evaluated histologically. Tamoxifen treatment decreased capsule thickness, decreased the number of  $\alpha$ SMA+ cells ( $477 \pm 156$  cells/mm control vs  $295 \pm 121$  cells/mm tamoxifen,  $p = 0.005$  unpaired *t* test), and decreased CD31+ cells ( $173.9 \pm 96.1$  cells/mm<sup>2</sup> control vs  $106.3 \pm 51.8$  cells/mm<sup>2</sup> tamoxifen,  $p = 0.043$  unpaired *t* test). There were similar amounts of pro- and anti-inflammatory macrophages (iNOS  $336.1 \pm 226.3$  cells/mm control vs  $290.6 \pm 104.2$  cells/mm tamoxifen,  $p > 0.999$  Mann–Whitney test and CD163  $136.6 \pm 76.4$  cells/mm control vs  $94.1 \pm 45.9$  cells/mm tamoxifen,  $p = 0.108$  unpaired *t* test). Tamoxifen treatment in the mouse silicone breast implant model decreased capsule formation through modulation of myofibroblasts, neovascularization, and collagen deposition. Tamoxifen may be useful for reducing or preventing capsule formation in clinical breast implantations.

## KEYWORDS

Breast Implant, Capsular Contracture, Tamoxifen, Mouse Model

## 1 | BACKGROUND

The formation of a capsule is a common foreign body reaction to all implanted materials, and the degree of capsule formation varies across patients, implant types, and procedure types. Capsules formed in response to foreign bodies are predominantly made up of inflammatory cells, fibroblasts, myofibroblasts, and collagen.<sup>1–3</sup> For breast

implant capsules, in particular, contracture of the capsule is a clinically significant diagnosis that results in pain, deformation of the implant, and need for surgical reoperation, occurring in 8%–20% of patients.<sup>4,5</sup> Capsular contracture is one of the most common causes of reoperation following implant-based breast reconstruction after cancer.<sup>6</sup> Capsular contracture is classified according to Baker grading from I to IV, with III and IV being more severe

**Abbreviations:** ER- $\alpha$ , estrogen receptor-alpha; ER- $\beta$ , estrogen receptor-beta; FBR, foreign body response; TGF- $\beta$ , transforming growth factor-beta;  $\alpha$ SMA, alpha-smooth muscle actin.

This is an open access article under the terms of the [Creative Commons Attribution-NonCommercial](https://creativecommons.org/licenses/by-nc/4.0/) License, which permits use, distribution and reproduction in any medium, provided the original work is properly cited and is not used for commercial purposes.

©2022 The Authors *FASEB BioAdvances* published by The Federation of American Societies for Experimental Biology.

and clinically significant.<sup>7</sup> Factors associated with the development of capsular contracture are time from implantation, with an increasing rate of contracture with time, and the thickness of the fibrous capsule that forms around the implant.<sup>1</sup> Risk factors for capsular contracture include radiation exposure, implant contamination or infection, smooth-walled implants, and subglandular placement of the implant as opposed to subpectoral placement; however, the primary cause of capsular contracture remains idiopathic in nature and it is unclear why some patients, but not others, develop clinically significant capsular contracture in comparable settings.<sup>8–10</sup>

Options for treatment of breast implant capsular contracture include surgical capsulectomy, an implant exchange (removal and replacement with a new implant), and altering the position where the implant is placed (i.e., from a subglandular plane to a subpectoral plane or in an adjacent “neopocket”).<sup>8</sup> Emphasis is aimed at the primary prevention of capsular contracture through modification of the surgical method, implant location, strategies to reduce the likelihood of implant contamination, and the use of textured implant surfaces.<sup>8,11</sup> Textured surfaces have been shown to decrease the formation of an implant capsule, with a proposed mechanism of decreasing collagen and cellular alignment in the fibrous capsule.<sup>12</sup> However, recent studies have found incidence of breast implant-associated lymphomas following textured surface implantation through a currently unknown mechanism.<sup>13–15</sup> Surface modifications and the addition of antibiotic and antifibrotic drugs have shown some success in preventing capsular contracture.<sup>6,9</sup> Antibiotics are utilized to address the biofilm hypothesis of capsule formation, which posits that capsule formation and contracture are exacerbated by the presence of a bacterial biofilm around the implant, which leads to long-term inflammation.<sup>9,16</sup> Additionally, recent research has focused on immune modulation in the formation of capsular contracture. TGF- $\beta$  and its role in the development and function of myofibroblasts have been implicated.<sup>17</sup> In previous studies, knock-out of periostin, an integrin ligand, in mice was shown to decrease the inflammatory markers as well as markers of fibrosis, including  $\alpha$ SMA and collagen I.<sup>18</sup> In addition, estrogen signaling has been noted to play a role in capsule formation, particularly with higher amounts of estrogen increasing the presence of myofibroblasts and collagen surrounding implants.<sup>3</sup> Correspondingly, capsular contracture is less common in patients on antiestrogen therapy.<sup>17</sup>

Tamoxifen, a selective estrogen receptor modulator, is clinically indicated in estrogen receptor-positive breast cancer treatment for which it has a potent antitumor effect.<sup>19</sup> However, tamoxifen has previously shown off-target efficacy in the reduction of fibrosis for skin scar formation in humans, particularly in terms of decreasing

the formation of hypertrophic scars in vivo and decreasing human fibroblast contraction of collagen matrices in vitro.<sup>20–22</sup> Tamoxifen has also been shown to reduce renal fibrosis after kidney injury in a rat model.<sup>23</sup>

Following the findings that estrogen modulation impacts breast implant capsular contracture rates, and that tamoxifen has functional efficacy against fibrotic tissue formation, we hypothesized that tamoxifen could be used to deliberately mitigate capsule formation following silicone breast implantation.

## 2 | METHODS

### 2.1 | Animal care and surgical implantation

All procedures and experiments involving the use of animals in this study were done in accordance with relevant guidelines and regulations with approval from the Abigail Wexner Research Institute (AWRI) at Nationwide Children’s Hospital Institutional Animal Care and Use Committee (IACUC) (Protocol AR12-00075).

Eight-week-old C57BL/6 or Beige (C57BL/6J-Lyst<sup>bg-J/J</sup>) female mice (Jackson Labs) ( $N = 10$ /group) were treated with daily tamoxifen or vehicle injections into the intraperitoneal cavity 1 week before surgery. Tamoxifen injections consisted of 75 mg/kg tamoxifen citrate (Sigma) in peanut oil (Sigma) with 10% ethanol (Sigma) to promote the dissolution of tamoxifen, while control injections consisted of only peanut oil and ethanol. Daily injections continued until the day of explantation, 2 weeks after implantation.

Silicone prostheses were cut from a solid sheet of medical implant-grade silicone (Goodfellow) using a 6 mm biopsy punch (Figure 1A). Prostheses were sterilized using 70% ethanol. Implants were submerged in 70% ethanol for 30 min and then allowed to air dry for 1 h within a sterilized cell culture hood, as previously described.<sup>24–28</sup>

Mice were anesthetized with a standard ketamine/xylazine cocktail. Fur was clipped and skin was prepped with betadine followed by alcohol pads. Silicone prostheses were implanted in the submammary plane, bilaterally, giving a total of 20 implants per experimental group (Figure 1B). Skin incisions were reapproximated with 6–0 nylon suture (Figure 1C). We specifically chose the submammary plane on the ventral surface, rather than dorsal back skin implantation, to more closely mimic the host microenvironment relevant to breast implantation and estrogen signaling.

After 2 weeks, mice were euthanized and the silicone prostheses were removed *en bloc* with all surrounding tissue, including the overlying skin for orientation (Figure 1D). Two weeks was chosen as the explantation time point based on previous data suggesting that this is a key timepoint in

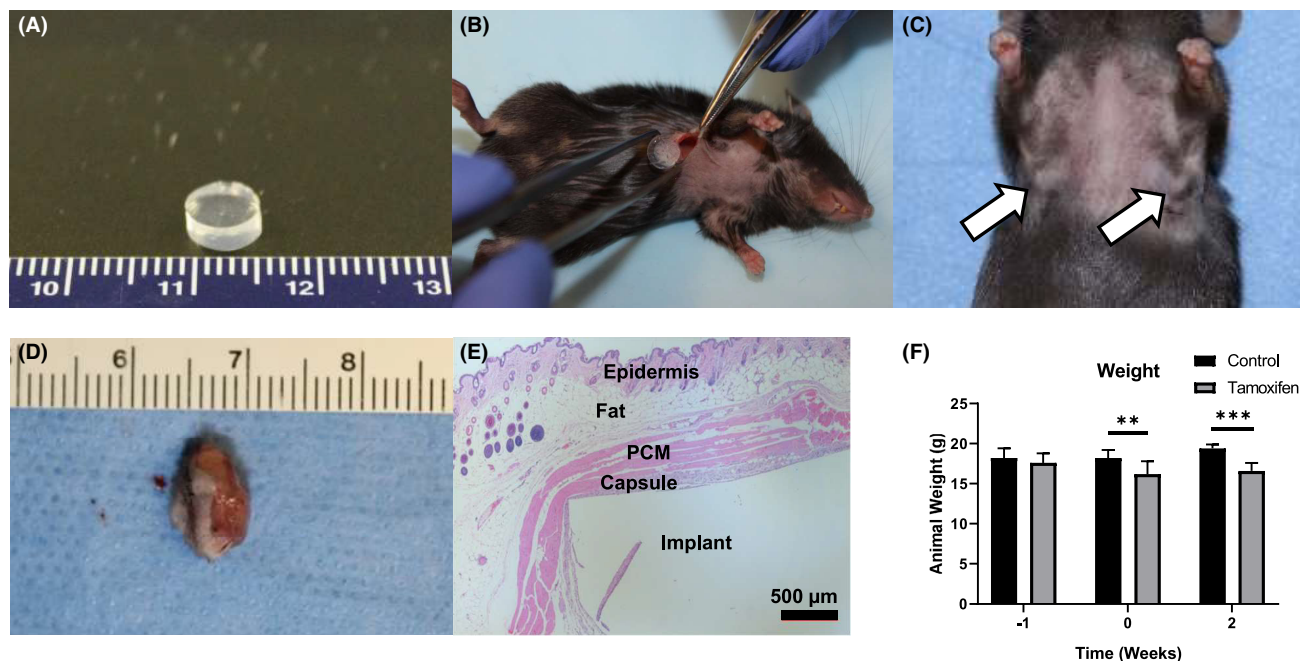


**FIGURE 1** Experimental design. Six millimeters diameter silicone implants (A) were implanted under the panniculus carnosus muscle (B) bilaterally (C) and explanted after 2 weeks. Implants and surrounding tissue were harvested *en bloc* (D) and sectioned for histology (E) scale bar 500  $\mu\text{m}$ . (F) Mouse weight in control animals and tamoxifen-treated animals over the experimentation time. Data compared with unpaired *t* tests or Mann–Whitney tests as appropriate (see text). \* $p < 0.05$ , \*\* $p < 0.01$ , \*\*\* $p < 0.001$ .

fibrous tissue development in mouse models.<sup>28,29</sup> Some animals accessed their incision causing implant exposure; however, all implant exposures occurred within 48 h after implantation. These samples were excluded from further analysis a priori owing to the potential confounding nature of bacterial contamination on capsule formation. After exclusion of implants that were exposed after surgery, 8/20 implants were available for the control group and 15/20 for the tamoxifen-treated group for further analysis.

## 2.2 | Histology

Explanted silicone pieces and surrounding capsules were fixed overnight in formaldehyde at 4°C and transitioned to 70% ethanol. Samples were then paraffin embedded and sectioned at 4  $\mu\text{m}$ . Samples were stained with H&E (Figure 1E) or Picro-Sirius Red. Immunohistochemistry sections were deparaffinized, rehydrated, and blocked for endogenous peroxidase activity (3%  $\text{H}_2\text{O}_2$  in  $\text{H}_2\text{O}$ ) and nonspecific background staining (3% normal goat serum in Background Sniper, BioCare Medical). Antigen retrieval was performed with citrate buffer (pH 6.0) or Tris-EDTA (pH 9.0) in a pressure cooker for 10 min, and slides were incubated for 30 min at room temperature with primary antibodies. Primary antibodies (all from Abcam) included  $\alpha$ -SMA (ab124964), CD31 (ab28364), CD68 (ab125212), iNOS (ab15323), CD163 (ab182422), Ki67

(ab15580), ER- $\alpha$  (ab271827), and ER- $\beta$  (ab3576). Primary antibody binding was detected by subsequent incubation with species-appropriate biotinylated IgG (Vector Laboratories), followed by streptavidin-horse radish peroxidase (Vector Laboratories) and chromogenic development with 3,3-diaminobenzidine (Vector Laboratories). Tissue sections were counterstained with Gill's hematoxylin (Vector Laboratories), slides were dehydrated, and a cover slip was placed. Slides were imaged on a Zeiss Axio Observer Z1 inverted microscope (Zeiss) and quantified using ImageJ (NIH).

Images were quantified by examining the area within the fibrous capsule on the side oriented with overlying skin at the midpoint of the implant to maintain consistency and remove potential variability from the dissection plane on the other side of the implant created at explantation. Due to the substantial differences in total capsular area, cellular histological stains were quantified using two methodologies, both as a percent of total cells within the capsule to determine differences in the makeup of the capsular tissue and as cells/mm of the implant surface to determine differences in the total amount of each cell type present.

## 2.3 | Statistics

All statistical analysis was performed in Prism 8.0 (GraphPad). Data were evaluated for outliers using



Grubb's test. Control and tamoxifen-treated groups were compared with unpaired *t* tests, except in cases where the equal variance assumption was violated, when the nonparametric Mann–Whitney test was utilized. A *p*-value of 0.05 was considered significant.

### 3 | RESULTS

#### 3.1 | Surgery and Follow-Up

While control and tamoxifen-treated groups had similar weights at the start of the injection period ( $18.2 \pm 1.2$  control vs  $17.6 \pm 1.2$  tamoxifen gram body weight,  $p = 0.279$  unpaired *t* test), the tamoxifen-treated animals had a lower body weight 1 week later at the date of surgery ( $18.2 \pm 1.0$  control vs  $16.2 \pm 1.6$  tamoxifen gram body weight,  $p < 0.01$  unpaired *t* test) and at the 2-week explant date ( $19.4 \pm 0.5$  control vs  $16.6 \pm 1.0$  tamoxifen gram body weight,  $p < 0.001$  unpaired *t*-test; Figure 1F).

#### 3.2 | Capsule thickness and cellular infiltration

Capsules were identified by histology as the plane of tissue formed between the implant surface and the panniculus carnosus muscle (Figure 2A). Implant capsules were significantly thinner in the tamoxifen-treated cohort ( $222 \pm 89 \mu\text{m}$  control vs  $132 \pm 49 \mu\text{m}$  tamoxifen,  $p = 0.0159$  Mann–Whitney test; Figure 2B), demonstrating a 59% reduction in capsule thickness. Cellularity of the capsules was found to be similar ( $3634 \pm 398$  cells/ $\text{mm}^2$  control vs  $3624 \pm 608$  cells/ $\text{mm}^2$  tamoxifen,  $p = 0.9684$  unpaired *t*-test; Figure 2C).

#### 3.3 | Collagen deposition

Total collagen surrounding the implants (Figure 2D) was significantly lower in the tamoxifen-treated animals compared with the untreated controls ( $79,312 \pm 22,991 \mu\text{m}^2$  control vs  $43,598 \pm 10,044 \mu\text{m}^2$  tamoxifen,  $p = 0.001$  Mann–Whitney test; Figure 2E). However, due to the differences

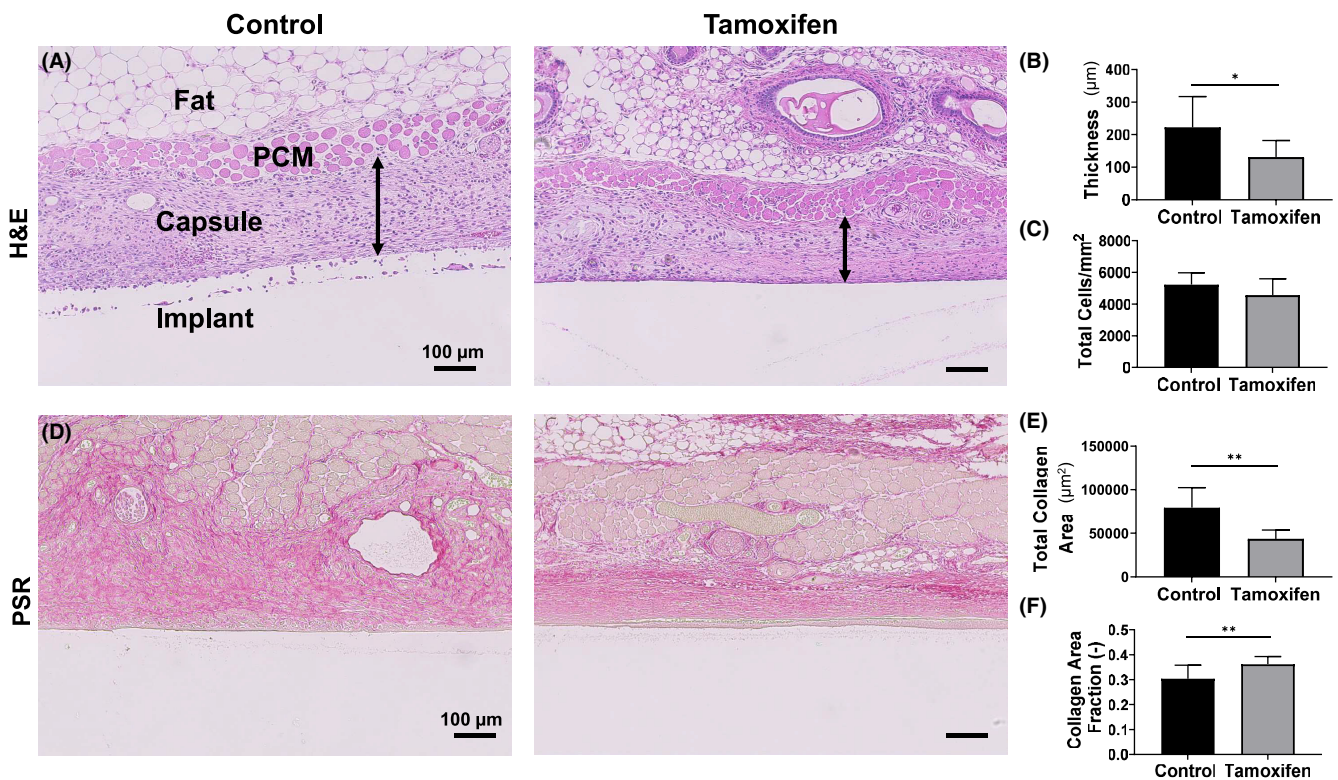


**FIGURE 2** Tamoxifen decreases capsule thickness and collagen deposition. (A) Representative H&E staining demonstrating the anatomical layers surrounding the implant, including the fibrous capsule, panniculus carnosus muscle (PCM), and subcutaneous fat. Double-sided arrow demonstrates the thickness of the capsule, (B) average thickness of the fibrous capsule at 2 weeks, (C) average total cellularity of the capsules, (D) representative picosirius red images of the capsules. Total collagen (E) and area fraction of collagen (F). Scale bars = 100  $\mu\text{m}$ . Data compared with unpaired *t* tests or Mann–Whitney tests as appropriate (see text). \* $p < 0.05$ , \*\* $p < 0.01$ , \*\*\* $p < 0.001$ .

in thickness between the capsules, there was a significantly higher area percent of collagen in the tamoxifen-treated group ( $30.4 \pm 5.8\%$  control vs  $36.2 \pm 3.1\%$  tamoxifen,  $p = 0.023$  Mann–Whitney test; **Figure 2F**).

### 3.4 | Estrogen receptors

Estrogen receptor- $\alpha$  (ER- $\alpha$ ) and estrogen receptor- $\beta$  (ER- $\beta$ ) were investigated, as tamoxifen is an estrogen analog that functions primarily through these targets. ER- $\alpha$  expression (**Figure 3A**) as a fraction of total cells was not affected by tamoxifen treatment ( $34.7 \pm 5.8\%$  control vs  $31.0 \pm 6.3\%$  tamoxifen,  $p = 0.184$  unpaired  $t$ -test; **Figure 3B**) but was lowered as a total cells/mm of capsular tissue ( $256.5 \pm 151.2$  cells/mm control vs  $107.0 \pm 39.8$  cells/mm tamoxifen,  $p = 0.003$  Mann–Whitney test; **Figure 3C**). ER- $\beta$  expression (**Figure 3D**) was not affected as measured by cellular fraction ( $31.6 \pm 5.0\%$  control vs  $36.8 \pm 7.5\%$  tamoxifen,  $p = 0.092$  unpaired  $t$  test; **Figure 3E**) nor total

cells/mm ( $169.3 \pm 102.9$  cells/mm control vs  $106.2 \pm 69.2$  cells/mm tamoxifen,  $p = 0.094$  unpaired  $t$  test; **Figure 3F**).

### 3.5 | Cellular proliferation

Ki-67 was used as a marker of cellular proliferation (**Figure 3G**). The cellular fraction of Ki-67+ cells was similar between groups ( $67.5 \pm 9.0\%$  control vs  $62.4 \pm 16.9\%$  tamoxifen,  $p = 0.440$  unpaired  $t$  test; **Figure 3H**); however, there were significantly fewer Ki-67+ cells/mm in the tamoxifen-treated mice ( $704 \pm 366$  cells/mm control vs  $324 \pm 125$  cells/mm tamoxifen,  $p = 0.003$  Mann–Whitney test; **Figure 3I**).

### 3.6 | Myofibroblasts

Alpha smooth muscle actin ( $\alpha$ SMA) was utilized as a marker of myofibroblasts within the implant capsule (**Figure 4A**). Although a similar percentage of total cells

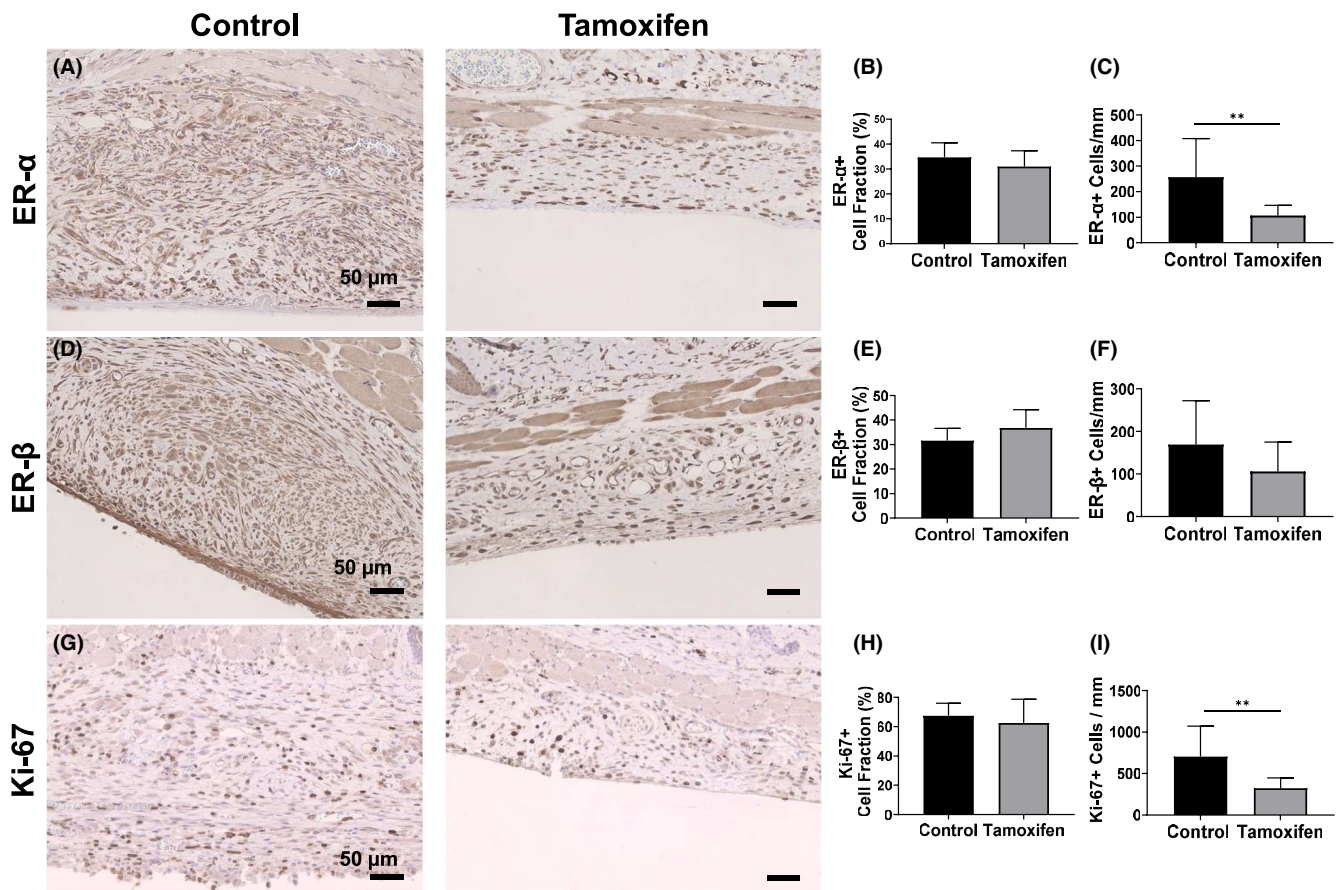


**FIGURE 3** Estrogen receptors and proliferation. (A) Representative histology of estrogen receptor- $\alpha$ , quantified as a cellular fraction (B) and total positive cells per mm (C). (D) Representative histology of estrogen receptor- $\beta$ , quantified as a cellular fraction (E) and total positive cells per mm (F). (G) Representative histology of proliferative marker Ki-67, quantified as cellular fraction (H) and total positive cells per mm (I). Scale bars = 50  $\mu$ m. Data compared with unpaired  $t$  tests or Mann–Whitney tests as appropriate (see text). \* $p < 0.05$ , \*\* $p < 0.01$ , \*\*\* $p < 0.001$ .



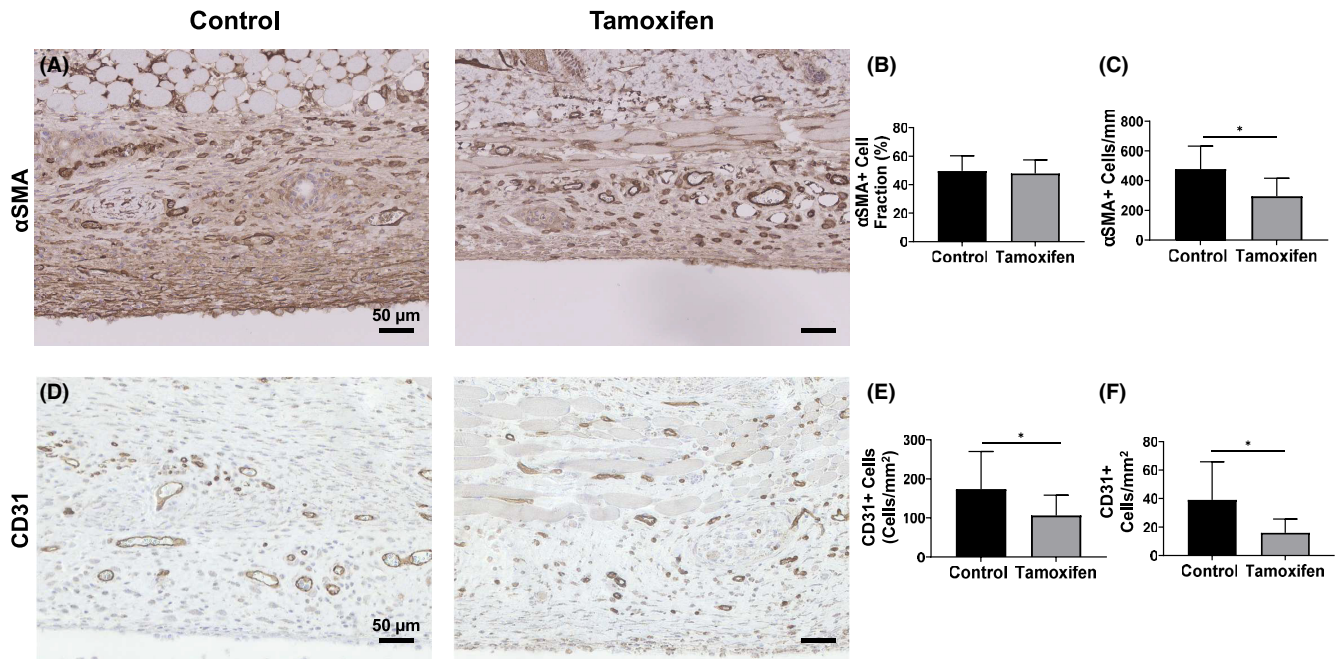


**FIGURE 4**  $\alpha$ SMA and CD31 expression. (A) Representative histology of myofibroblast marker  $\alpha$ SMA, quantified as a cellular fraction (B) and total positive cells per mm (C). (D) Representative histology of endothelial cell marker CD31, quantified as cells per mm<sup>2</sup> (E) and cells per mm (F). Scale bars = 50  $\mu$ m. Data compared with unpaired t tests or Mann–Whitney tests as appropriate (see text). \* $p$  < 0.05, \*\* $p$  < 0.01, \*\*\* $p$  < 0.001.

$\alpha$ SMA+ (49.6  $\pm$  10.6% control vs 47.9  $\pm$  9.5% tamoxifen,  $p$  = 0.690 unpaired t-test; **Figure 4B**), the linear density of  $\alpha$ SMA+ cells was significantly reduced in tamoxifen-treated animals relative to controls (477  $\pm$  156 cells/mm control vs 295  $\pm$  121 cells/mm tamoxifen,  $p$  = 0.005 unpaired t-test; **Figure 4C**).

### 3.7 | Neovascularization

CD31, a marker of endothelial cells, was used to identify the formation of blood vessels within the capsule (**Figure 4D**). Tamoxifen-treated mice were found to have significantly fewer cells/mm<sup>2</sup> than control animals (173.9  $\pm$  96.1 cells/mm<sup>2</sup> control vs 106.3  $\pm$  51.8 cells/mm<sup>2</sup> tamoxifen,  $p$  = 0.043 unpaired t-test; **Figure 4E**) and fewer total CD31+ cells (39.1  $\pm$  26.7 cells/mm control vs 15.9  $\pm$  9.7 cells/mm,  $p$  = 0.040 Mann–Whitney test; **Figure 4F**).

### 3.8 | Macrophages

Macrophage infiltration of the capsule was investigated using CD68 (**Figure 5A**). There was no difference in the cellular fraction of CD68 (62.1  $\pm$  19.1% control vs 55.9  $\pm$  16.0% tamoxifen,  $p$  = 0.419 unpaired t-test; **Figure 5B**). The linear density of CD68+ cells surrounding the tamoxifen implants was lower than the control

implants (718.9  $\pm$  391.2 cells/mm control vs 303.3  $\pm$  136.5 cells/mm,  $p$  = 0.011 Mann–Whitney test; **Figure 5C**).

Pro-inflammatory and anti-inflammatory macrophages were labeled with iNOS (**Figure 5D**) and CD163 (**Figure 5E**), respectively. The cellular fractions of both iNOS and CD163 were higher in tamoxifen-treated animals (iNOS 31.6  $\pm$  18.1% control vs 60.6  $\pm$  12.6% tamoxifen,  $p$  < 0.001, unpaired t-test; **Figure 5F** and CD163 14.7  $\pm$  7.2% control vs 29.1  $\pm$  8.4% tamoxifen,  $p$  < 0.001, unpaired t-test; **Figure 5G**). There were no differences seen in the total number of cells with positivity for iNOS or CD163 between-groups (iNOS 336.1  $\pm$  226.3 cells/mm control vs 290.6  $\pm$  104.2 cells/mm tamoxifen,  $p$  > 0.999 Mann–Whitney test; **Figure 5H** and CD163 136.6  $\pm$  76.4 cells/mm control vs 94.1  $\pm$  45.9 cells/mm tamoxifen,  $p$  = 0.108 unpaired t test; **Figure 5I**).

### 3.9 | Effect of Beige mutation on capsular formation

We compared the effects of innate immunodeficiency to tamoxifen treatment to delineate potential contributions of immune modulation versus antiproliferative effects of tamoxifen. We utilized the beige mouse as a model of innate immunodeficiency.<sup>30–32</sup> Beige mice were similarly treated with vehicle injections identical to control animals. Similar to the control and tamoxifen-treated

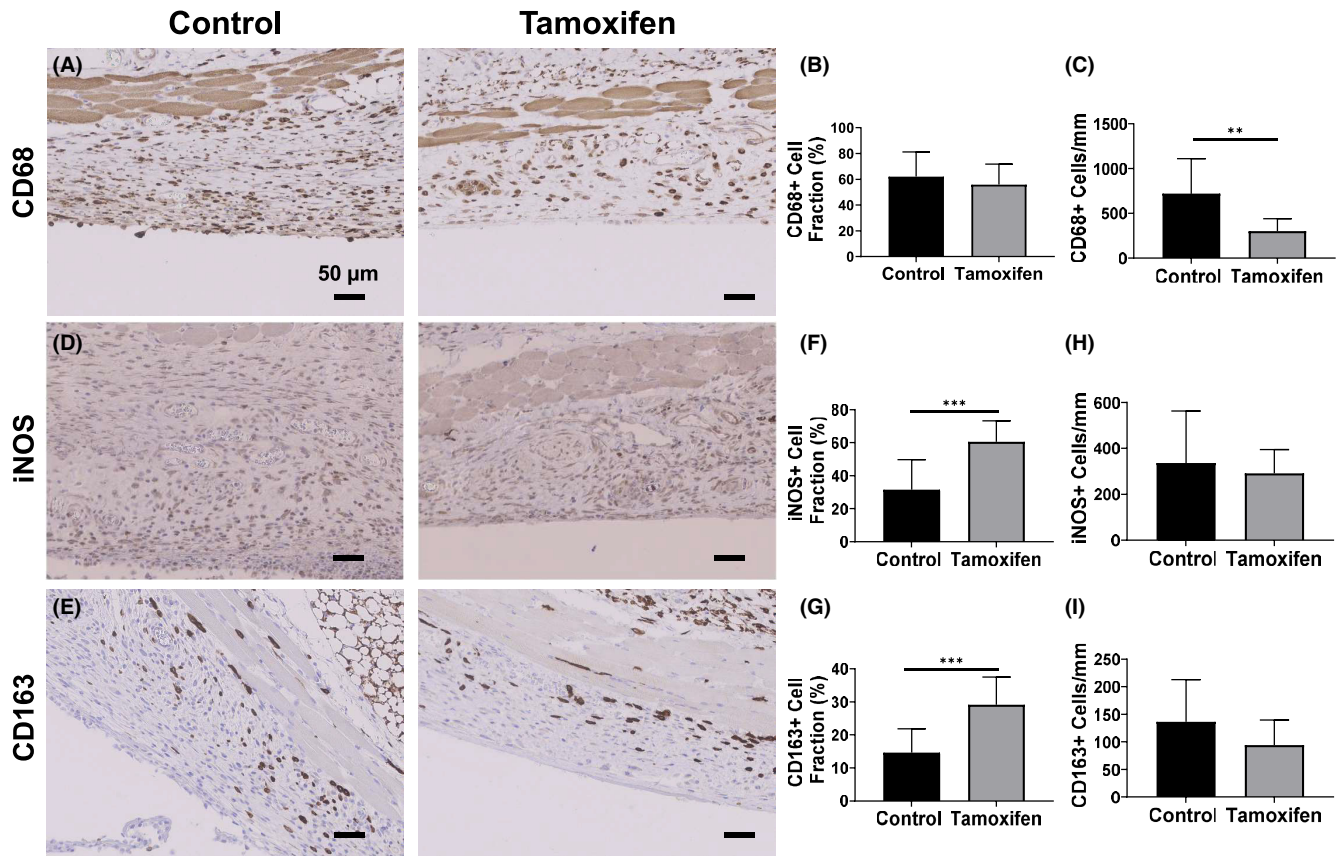


**FIGURE 5** Macrophage response. A) Representative histology of macrophage marker CD68, quantified as a cellular fraction (B) and total positive cells per mm (C). Representative imaging of pro-inflammatory macrophage marker iNOS (D) and anti-inflammatory macrophage marker CD163 (E) was also shown, with quantifications performed as a cellular fraction (F and G) and as total cells per mm (H and I) for iNOS and CD163, respectively. Scale bars = 50  $\mu\text{m}$ . Data compared with unpaired *t* tests or Mann–Whitney tests as appropriate (see text). \* $p < 0.05$ , \*\* $p < 0.01$ , \*\*\* $p < 0.001$ .

groups, 10 out of 20 beige implants were removed from the study due to implant exposure over the first 48 h post-implantation. Beige mice had comparable capsule thickness to control mice ( $222 \pm 95 \mu\text{m}$  control vs  $190 \pm 78 \mu\text{m}$  beige,  $p = 0.436$  unpaired *t*-test). Most histological markers did not exhibit differences between control and beige animals; however, there was a decreased amount of collagen deposition in beige animals compared with controls ( $79,312 \pm 22,991 \mu\text{m}^2$  control vs  $51,400 \pm 16,951 \mu\text{m}^2$  beige,  $p = 0.016$ , Mann–Whitney test; Figure S1). Interestingly, there were no statistical differences between the beige animals and the tamoxifen-treated animals in any histological markers. Overall, the beige model appeared to have a minor trend toward decreasing fibrous capsule formation, but to a lesser extent than tamoxifen treatment.

#### 4 | DISCUSSION

This study demonstrates the potential utility of tamoxifen for reducing fibrous capsule formation in a mouse model

of silicone breast implantation. Total fibrous capsule thickness and collagen deposition were significantly reduced in tamoxifen-treated mice relative to controls. Due to differences in total tissue formed around implants of identical size, comparison of total cells encasing the implant as well as the average composition of the deposited tissue for each marker studied was crucial for understanding the noted histological differences.

In this study, tamoxifen behaved as a potent antiproliferative or anticellular-infiltrative agent to reduce capsule formation around a foreign body, and this effect appeared to be more contributory than immunomodulation. Tamoxifen is a known antiproliferative agent in estrogen receptor-positive breast cancer, in other tumors, such as desmoid tumors, and fibrosing conditions.<sup>22,33–35</sup> In rats, tamoxifen has been shown to decrease fibroblast viability, proliferation, epidural fibrosis, and dural thickness following laminectomy.<sup>36,37</sup> Tamoxifen also acts as an antifibrotic treatment for patients with idiopathic retroperitoneal fibrosis.<sup>38,39</sup> Additionally, tamoxifen has a potent antiangiogenic effect, which was also validated by

our current study.<sup>40,41</sup> These findings are relevant because higher Baker grades of capsular contracture are associated with greater levels of angiogenesis.<sup>3</sup>

Although the total numbers of CD68+ cells were decreased in tamoxifen-treated mice, total amounts of both pro-inflammatory iNOS+ and anti-inflammatory CD163+ macrophages were not affected. This difference may be explained by the promiscuity of the CD68 cellular marker, which stains not only macrophages but also fibroblasts.<sup>42,43</sup> Indeed, myofibroblasts, denoted by  $\alpha$ SMA, were decreased in tamoxifen treatment and may better explain the differences in CD68 staining. These results suggest that tamoxifen modulates the fibrous capsule formation by directly inhibiting the infiltration of fibroblastic cells and total deposition of collagen, without a significant effect on the inflammatory cell response. To further evaluate this possible modulation, correlations between  $\alpha$ -SMA expression and capsule thickness to ER- $\alpha/\beta$  were performed (Figure S2). Although the statistical power of these regressions remains low due to sample size, regressions suggest a possible interaction between the variables, in particular, between ER- $\alpha$  and  $\alpha$ SMA expression within the formed capsules. This is further supported by the fact that we saw little modulation of capsule formation when the same technique was applied to a mouse model of innate immunodeficiency, the beige mouse.

In this study, tamoxifen treatment was shown to have an effect on ER- $\alpha$  expression but not on ER- $\beta$  expression. This is similar to previous studies, which have shown that tamoxifen's primary target is ER- $\alpha$ , with additional relatively low interaction with ER- $\beta$ .<sup>44,45</sup> Tamoxifen has known mechanisms of action both directly through the hormonal estrogen receptors as well as nonhormonal pathways. It is important to recognize that the hormonal effects of estrogen, as well as estrogen analogs such as tamoxifen, are tissue specific. For example, while tamoxifen has shown utility in decreasing fibrosis in this study as well as in studies of retroperitoneal fibrosis and keloid formation, tamoxifen use has been associated with increased fibrosis in lung tissue and steatohepatitis in liver tissue.<sup>22,39,46,47</sup> Nonhormonal mechanisms of action of tamoxifen are believed to act through the TGF- $\beta$  pathway, although the precise mechanism is unknown.<sup>48</sup> Tamoxifen has also been shown to have sex-specific effects on the wound-healing pathways of mice.<sup>49</sup> These mechanisms of action are important considerations in the context of our findings. Since estrogen receptor levels and response to tamoxifen vary with species and sex, the external validity of the effects at tamoxifen at decreasing fibrosis in humans should be further evaluated. Clinically, tamoxifen has a potent antitumor effect in estrogen receptor-positive breast cancer but is carcinogenic to vaginal and cervical tissue.<sup>50</sup> These known clinical complications should be noted in the further development of this technology, as systemic application of tamoxifen opens the

possibility for off-target systemic effects.<sup>51</sup> To this end, systemic treatment with tamoxifen and its associated side effects could potentially be avoided through the use of local release of tamoxifen's active metabolite endoxifen, which has shown 30- to 100-fold greater potency than tamoxifen when delivered orally or through IV injections in mice.<sup>52</sup> Future studies utilizing longer time periods of evaluation as well as large animal models are warranted to better evaluate the effectiveness of the tamoxifen treatments.

The limitations of this study should be noted. Due to animal interference with the surgical site and exposure of implants, several experimental samples had to be discarded, reducing the total number of included samples in the study and decreasing the possible statistical power. However, in the outcomes described, statistical power remained sufficient despite this limitation. In this study, tamoxifen treatment was associated with a decrease in animal weight over the total 3 weeks of tamoxifen treatment. This result provides a potential confounder to experimental results, as cachexia and low weight are known comorbidities to surgical outcomes and have effects on wound-healing properties.<sup>53,54</sup> However, we have previously reported that tamoxifen's effects on reducing collagen formation and cellular infiltration into a tissue-engineered vascular graft in a murine model were due to tamoxifen itself and not the associated weight loss.<sup>49</sup> The contribution of bacterial biofilm to capsular formation and contracture is a valid phenomenon.<sup>55</sup> This work did not evaluate the contribution of potential bacterial contamination on individual implants; however, all surgeries were performed in accordance with the aseptic technique and utilized identical sterile implants. Future studies may also require the evaluation of alternative sterilization procedures, such as ethylene oxide, gas plasma, or radiation.

Last, as with all studies performed in animal models, careful critique must be employed in extrapolating findings to human clinical applications, as animal models have several known and unknown differences from human model counterparts.<sup>56</sup>

## 5 | CONCLUSION

Herein we demonstrate proof of principle that tamoxifen or its active metabolites may be beneficial in reducing the development of fibrous capsule formation around breast implants.

### AUTHOR CONTRIBUTIONS

Blum, Breuer, and Barker designed the research; Blum, Mirhaidari, Zbinden, and Barker performed the research; Blum, Mirhaidari, and Zbinden analyzed data; and Blum and Barker wrote the manuscript.



Kevin Blum: conceptualization (supporting); investigation (equal); formal analysis (lead); writing – original draft (lead); writing – review and editing (equal). Gabriel Mirhaidari: investigation (supporting); formal analysis (supporting); writing – review and editing (supporting). Jacob Zbinden: investigation (supporting); formal analysis (supporting); writing – review and editing (supporting). Christopher Breuer: conceptualization (supporting); methodology (supporting); writing – review and editing (equal). Jenny Barker: conceptualization (lead); methodology (lead); investigation (equal); writing – original draft (supporting); writing – review and editing (equal).

## ACKNOWLEDGMENTS

This work was funded by the Dr. Stuart S. and Letitia Roberts Collaborative Research Award from the Ohio State University. KMB was supported by the Tau Beta Pi 35th Centennial Fellowship. JCB was supported by the NIH F32HL144120, NIH T32AI106704, and the Ohio State University President's Postdoctoral Scholar Program.

## CONFLICT OF INTEREST

The authors state explicitly that there are no conflict of interest in connection with this article.

## ORCID

Kevin M. Blum  <https://orcid.org/0000-0002-8346-629X>

Jenny C. Barker  <https://orcid.org/0000-0002-1517-5124>

## REFERENCES

- Bui JM, Perry T, Ren CD, Nofrey B, Teitelbaum S, Van Epps DE. Histological characterization of human breast implant capsules. *Aesthetic Plast Surg*. 2015;39(3):306-315.
- Anderson JM, Rodriguez A, Chang DT. Foreign body reaction to biomaterials. *Semin Immunol*. 2008;20(2):86-100.
- Segreto F, Carotti S, Marangi GF, et al. The role of angiogenesis, inflammation and estrogen receptors in breast implant capsules development and remodeling. *J Plast Reconstr Aesthet Surg*. 2018;71(5):637-643.
- Adams WP, Haydon MS, Raniere J, et al. A rabbit model for capsular contracture: development and clinical implications. *Plast Reconstr Surg* 2006;117(4):1214-9; discussion 20-1.
- Gutowksi KA, Mesna GT, Cunningham BL. Saline-filled breast implants: a plastic surgery educational foundation multicenter outcomes study. *Plast Reconstr Surg*. 1997;100(4):1019-1027.
- Shin BH, Kim BH, Kim S, Lee K, Choy YB, Heo CY. Silicone breast implant modification review: overcoming capsular contracture. *Biomater Res*. 2018;22:37.
- Spear SL, Baker JL. Classification of capsular contracture after prosthetic breast reconstruction. *Plast Reconstr Surg* 1995;96(5):1119-23; discussion 24.
- Wan D, Rohrich RJ. Revisiting the management of capsular contracture in breast augmentation: a systematic review. *Plast Reconstr Surg*. 2016;137(3):826-841.
- Mempin M, Hu H, Chowdhury D, Deva A, Vickery K. The A, B and C's of silicone breast implants anaplastic large cell lymphoma, biofilm and capsular contracture. *Materials (Basel)*. 2018;11(12):2393.
- Haran O, Bracha G, Tiosano A, et al. Postirradiation capsular contracture in implant-based breast reconstruction: management and outcome. *Plast Reconstr Surg*. 2021;147(1):11-19.
- Headon H, Kasem A, Mokbel K. Capsular contracture after breast augmentation: an update for clinical practice. *Arch Plast Surg*. 2015;42(5):532-543.
- Fischer S, Hirche C, Reichenberger MA, et al. Silicone implants with smooth surfaces induce thinner but denser fibrotic capsules compared to those with textured surfaces in a rodent model. *PLoS One*. 2015;10(7):e0132131.
- Coleman DJ, Foo IT, Sharpe DT. Textured or smooth implants for breast augmentation? A prospective controlled trial. *Br J Plast Surg*. 1991;44(6):444-448.
- Hwang MJ, Brown H, Murrin R, Momtahan N, Sterne GD. Breast implant-associated anaplastic large cell lymphoma: a case report and literature review. *Aesthet Plast Surg*. 2015;39(3):391-395.
- Chen VW, Hoang D, Clancy S. Breast implant-associated bilateral B-cell lymphoma. *Aesthet Surg J*. 2020;40(2):NP52-NP58.
- Ajdic D, Zoghbi Y, Gerth D, Panthaki ZJ, Thaller S. The relationship of bacterial biofilms and capsular contracture in breast implants. *Aesthet Surg J*. 2016;36(3):297-309.
- Persichetti P, Segreto F, Carotti S, Marangi GF, Tosi D, Morini S. Oestrogen receptor-alpha and -beta expression in breast implant capsules: experimental findings and clinical correlates. *J Plast Reconstr Aesthet Surg*. 2014;67(3):308-315.
- Bae HS, Son HY, Lee JP, Chang H, Park JU. The role of Periostin in capsule formation on silicone implants. *Biomed Res Int*. 2018;2018:3167037.
- Kelley BP, Valero V, Yi M, Kronowitz SJ. Tamoxifen increases the risk of microvascular flap complications in patients undergoing microvascular breast reconstruction. *Plast Reconstr Surg*. 2012;129(2):305-314.
- Mousavi SR, Raaiszadeh M, Aminseresh M, Behjoo S. Evaluating tamoxifen effect in the prevention of hypertrophic scars following surgical incisions. *Dermatol Surg*. 2010;36(5):665-669.
- Payne WG, Ko F, Anspaugh S, Wheeler CK, Wright TE, Robson MC. Down-regulating causes of fibrosis with tamoxifen: a possible cellular/molecular approach to treat rhinophyma. *Ann Plast Surg*. 2006;56(3):301-305.
- Gragani A, Warde M, Furtado F, Ferreira LM. Topical tamoxifen therapy in hypertrophic scars or keloids in burns. *Arch Dermatol Res*. 2010;302(1):1-4.
- Dellé H, Rocha JR, Cavaglieri RC, Vieira JM, Malheiros DM, Noronha IL. Antifibrotic effect of tamoxifen in a model of progressive renal disease. *J Am Soc Nephrol*. 2012;23(1):37-48.
- Zhang YZ, Bjursten LM, Freij-Larsson C, Kober M, Wesslén B. Tissue response to commercial silicone and polyurethane elastomers after different sterilization procedures. *Biomaterials*. 1996;17(23):2265-2272.
- Lacerda VA, Pereira LO, Hirata JUNIOR, Perez CR. Evaluation of two disinfection/sterilization methods on silicon rubber-based composite finishing instruments. *Am J Dent*. 2015;28(6):337-341.
- Bhaskar P, Bosworth LA, Wong R, et al. Cell response to sterilized electrospun poly( $\epsilon$ -caprolactone) scaffolds to aid tendon regeneration in vivo. *J Biomed Mater Res A*. 2017;105(2):389-397.
- Hallfeldt KK, Stützel H, Puhmann M, Kessler S, Schweiberer L. Sterilization of partially demineralized bone matrix: the effects

- of different sterilization techniques on osteogenetic properties. *J Surg Res.* 1995;59(5):614-620.
28. Smith PN, Palenik CJ, Blanchard SB. Microbial contamination and the sterilization/disinfection of surgical guides used in the placement of endosteal implants. *Int J Oral Maxillofac Implants.* 2011;26(2):274-281.
  29. Hibino N, Yi T, Duncan DR, et al. A critical role for macrophages in neovessel formation and the development of stenosis in tissue-engineered vascular grafts. *FASEB J.* 2011;25(12):4253-4263.
  30. Hibino N, Mejias D, Pietris N, et al. The innate immune system contributes to tissue-engineered vascular graft performance. *FASEB J.* 2015;29(6):2431-2438.
  31. Zbinden JC, Blum KM, Berman AG, et al. Effects of braiding parameters on tissue engineered vascular graft development. *Adv Healthc Mater.* 2020;9(24):e2001093.
  32. Spritz RA. Genetic defects in Chediak-higashi syndrome and the beige mouse. *J Clin Immunol.* 1998;18(2):97-105.
  33. Bardon S, Vignon F, Derocq D, Rochefort H. The antiproliferative effect of tamoxifen in breast cancer cells: mediation by the estrogen receptor. *Mol Cell Endocrinol.* 1984;35(2-3):89-96.
  34. Kinzbrunner B, Ritter S, Domingo J, Rosenthal CJ. Remission of rapidly growing desmoid tumors after tamoxifen therapy. *Cancer.* 1983;52(12):2201-2204.
  35. Hansmann A, Adolph C, Vogel T, Unger A, Moeslein G. High-dose tamoxifen and sulindac as first-line treatment for desmoid tumors. *Cancer.* 2004;100(3):612-620.
  36. Wang S, Li X, Yan L, et al. Tamoxifen inhibits fibroblast proliferation and prevents epidural fibrosis by regulating the AKT pathway in rats. *Biochem Biophys Res Commun.* 2018;497(4):937-942.
  37. Ozturk Y, Bozkurt I, Yaman ME, et al. Histopathologic analysis of tamoxifen on epidural fibrosis. *World Neurosurg.* 2018;111:e941-e948.
  38. Ergun I, Keven K, Canbakan B, Ekmekci Y, Erbay B. Tamoxifen in the treatment of idiopathic retroperitoneal fibrosis. *Int Urol Nephrol.* 2005;37(2):341-343.
  39. van der Bilt FE, Hendriksz TR, van der Meijden WA, Brillman LG, van Bommel EF. Outcome in patients with idiopathic retroperitoneal fibrosis treated with corticosteroid or tamoxifen monotherapy. *Clin Kidney J.* 2016;9(2):184-191.
  40. Bogush T, Dudko E, Bogush E, Polotsky B, Tjulandin S, Davydov M. Tamoxifen non-estrogen receptor mediated molecular targets. *Oncol Rev.* 2012;6(2):e15.
  41. Helmestam M, Andersson H, Stavreus-Evers A, Brittebo E, Olovsson M. Tamoxifen modulates cell migration and expression of angiogenesis-related genes in human endometrial endothelial cells. *Am J Pathol.* 2012;180(6):2527-2535.
  42. Gottfried E, Kunz-Schughart LA, Weber A, et al. Expression of CD68 in non-myeloid cell types. *Scand J Immunol.* 2008;67(5):453-463.
  43. Inoue T, Plieth D, Venkov CD, Xu C, Neilson EG. Antibodies against macrophages that overlap in specificity with fibroblasts. *Kidney Int.* 2005;67(6):2488-2493.
  44. Grubberger-Saal SK, Bendahl PO, Saal LH, et al. Estrogen receptor beta expression is associated with tamoxifen response in ERalpha-negative breast carcinoma. *Clin Cancer Res.* 2007;13(7):1987-1994.
  45. Xue M, Zhang K, Mu K, et al. Regulation of estrogen signaling and breast cancer proliferation by an ubiquitin ligase TRIM56. *Oncogenesis.* 2019;8(5):30.
  46. Bentzen SM, Skoczylas JZ, Overgaard M, Overgaard J. Radiotherapy-related lung fibrosis enhanced by tamoxifen. *J Natl Cancer Inst.* 1996;88(13):918-922.
  47. Nishino M, Hayakawa K, Nakamura Y, Morimoto T, Mukaiharu S. Effects of tamoxifen on hepatic fat content and the development of hepatic steatosis in patients with breast cancer: high frequency of involvement and rapid reversal after completion of tamoxifen therapy. *Am J Roentgenol.* 2003;180(1):129-134.
  48. Chen H, Tritton TR, Kenny N, Absher M, Chiu JF. Tamoxifen induces TGF-beta 1 activity and apoptosis of human MCF-7 breast cancer cells in vitro. *J Cell Biochem.* 1996;61(1):9-17.
  49. Blum K, Roby L, Zbinden J, et al. Sex and tamoxifen confound murine experimental studies in cardiovascular tissue engineering. *Nat Sci Rep.* 2021;11(1):8037.
  50. Varras M, Polyzos D, Akrivis C. Effects of tamoxifen on the human female genital tract: review of the literature. *Eur J Gynaecol Oncol.* 2003;24(3-4):258-268.
  51. Shehata M, van Amerongen R, Zeeman AL, Giraddi RR, Stingl J. The influence of tamoxifen on normal mouse mammary gland homeostasis. *Breast Cancer Res.* 2014;16(4):411.
  52. Reid JM, Goetz MP, Buhrow SA, et al. Pharmacokinetics of endoxifen and tamoxifen in female mice: implications for comparative in vivo activity studies. *Cancer Chemother Pharmacol.* 2014;74(6):1271-1278.
  53. Ng MF. Cachexia – an intrinsic factor in wound healing. *Int Wound J.* 2010;7(2):107-113.
  54. Hunt BJ. Hemostasis at extremes of body weight. *Semin Thromb Hemost.* 2018;44(7):632-639.
  55. Moon DJ, Deva AK. Adverse events associated with breast implants: the role of bacterial infection and biofilm. *Clin Plast Surg.* 2021;48(1):101-108.
  56. Grada A, Mervis J, Falanga V. Research techniques made simple: animal models of wound healing. *J Invest Dermatol.* 2018;138(10):2095-105.e1.

## SUPPORTING INFORMATION

Additional supporting information can be found online in the Supporting Information section at the end of this article.

**How to cite this article:** Blum KM, Mirhaidari GJM, Zbinden JC, Breuer CK, Barker JC. Tamoxifen reduces silicone implant capsule formation in a mouse model. *FASEB BioAdvances.* 2022;4:638-647. doi: [10.1096/fba.2022-00036](https://doi.org/10.1096/fba.2022-00036)